STUDIES OF ROTORCRAFT AGILITY AND MANEUVERABILITY

H. C. Curtiss, Jr., Princeton University

and

George Price, Sikorsky Aircraft

UNITED TECHNOLOGIES CORPORATION

ABSTRACT

Current rotorcraft maneuverability models are derived from high speed fixed-wing simulations and do not accurately represent the unique maneuvers or limits associated with rotorcraft. Two simplified rotorcraft models are derived which are valid at low speeds and in uncoordinated flight and can be used to examine some of the fundamental aspects of maneuverability and agility. The approach taken is to separate the total induced power and propulsive power above that for steady level flight from the usual expression for total power required. The sum of the induced and propulsive power is then expressed in terms of the horizontal and vertical accelerations in the maneuvering state. Maneuver limits can then be calculated in terms of vehicle design parameters. At low speeds, the attainable levels of acceleration, deceleration, climb, and load factor depend on available control power, control rates, and pilot limits as well as installed power. Because of the direct connection between body attitude and acceleration, it is suggested that an auxiliary thruster would increase vehicle agility, especially at low speeds.

1. Introduction

Accurate assessments of agility and maneuverability are desired because of their importance in defining rotorcraft effectiveness in nap-of-earth (NOE) flight, air-to-air combat, and their impact on overall pilot workload. Of particular interest to Sikorsky Aircraft as a manufacturer and systems integrator is the relationship of these characteristics to vehicle design parameters and to the design optimization process. In lieu of full scale flight testing, simulations of varying levels of complexity are used to predict the combat effectiveness of a conceptual design. It is of interest, therefore, to consider the applicability and limitations of models of varying complexity in order to pursue the optimization process.

Projected roles for helicopters on future battlefields demand increased levels of survivability and offensive mission capability. The high density of lethal, ground-based threat systems, as well as the presence of numerous threat helicopter forces, dictate a maximum use of terrain masking in NOE flight to avoid detection. Once a helicopter is committed to an engagement, superior performance, weapons and sensor capabilities will be relied upon to provide the margin for success.

Simply adding armor and increasing the weight of the mission equipment package is not an optimal solution. A balance must be found between air vehicle performance, weapon characteristics, and sensor capabilities to optimize the design as an integrated system. Because these vehicle attributes drive the ultimate weight and cost of a design it is important to identify the required levels of subsystem perform-

ance during the design optimization process. As a result of the increasing emphasis on NOE flight and air-to-air combat, attention has recently turned to a better understanding of aircraft maneuverability and agility. This is especially true in the low speed flight regime where rotorcraft can exploit their unique characteristics.

Combat simulation provides a means of supporting design trade-off analyses by integrating the contributions of all subsystems into an aggregate measure of system effectiveness. It can be used to quantify the improvements required in vehicle design and weapon or sensor performance, evaluate likely engagement conditions, explore tactics, and identify the optimum mix of vehicle and mission equipment package performance. Such simulation results are often subject to validation through flight testing. Project D-318, sponsored by the U.S. Army Applied Technology Laboratories and the U.S. Navy Test Pilot School, was a field trial simulating close air combat engagements between OH-58, AH-1S, UH-60A and H-76 helicopters. Pilots found that low speed, uncoordinated maneuvers played a major part in maintaining weapons tracking of targets.

Current helicopter battlefield simulations are extensions of three-degree of freedom point-mass models developed for fixed-wing design evaluation. They are primarily valid at speeds above 60 knots, assume coordinated flight, and employ conventional fixed-wing maneuvers. At higher speeds this is a satisfactory approximation for helicopter flight. However, speeds in the NOE environment are typically between hover and 40 knots. The unique flying characteristics of the helicopter open up a new set of tactical maneuver choices not available with a fixed-wing design. These include slowing to a hover while tracking a target with a pedal turn, forward flight with large sideslip angles to increase the off-axis weapons pointing envelope, sideward flight and rearward flight. This paper discusses two simplified models which are valid at low speeds and can be used to examine some of the fundamental aspects of maneuverability and agility.

2. Maneuverability

Maneuverability is taken to be associated with the limiting flight paths that are possible for a given rotorcraft. Agility is associated with the time required to establish the specific flight path. In the sections that follow, the nature of these limits is examined and the factors associated with achieving these limits are considered. The boundaries on the flight envelope of a helicopter arise from a number of sources, including: rotor design limits, available control power, acceptable body attitudes and rates, and installed power. The limiting behavior of rotorcraft as governed by installed power and control will be the focus of this paper. Rotor design limits will not be considered.

3. Maneuverability Models

Mathematical models of maneuvering flight for rotorcraft tend to fall into two categories: highly simplified and highly complex. On one hand, highly simplified point-mass models (such as found in References (1) and (2)) assume that all maneuvers are coordinated and that coordination corresponds to zero sideslip; the case for a fixed wing aircraft. In reality, coordinated flight of a helicopter does not occur at zero sideslip, even in steady flight. Furthermore, the restriction to coordinated flight eliminates many maneuvers unique to rotorcraft that may be employed at low speeds. On the other hand,

highly complex simulations are available which give limited physical insight into the important vehicle parameters that determine agility and maneuverability.

This paper describes and discusses models falling between the above extremes with sufficient complexity to show the essential features of rotorcraft agility and maneuverability. Considerable attention is devoted to some of the unique maneuvers that can be performed in low speed flight.

4. Aerodynamic Force Limits

The aerodynamic force limits of a flight vehicle are conveniently examined in a wind axis frame. The equations of motion describing the motion of the velocity vector can be written as:

$$\begin{aligned} \dot{V} + g \sin\gamma &= g\, \eta_{xw} \\ V\dot{\gamma} + g \cos\gamma &= g\, \eta_{zw} \cos\phi_w \\ V\dot{\chi} &= g\, \frac{\eta_{zw} \sin\phi_w}{\cos\gamma} \end{aligned} \tag{1}$$

χ and γ determine the orientation of the velocity V as shown in Figure 1. These equations of motion have been used in a number of studies of helicopter maneuverability (References 1 and 2). It has been assumed that there is no aerodynamic sideforce on the vehicle ($\eta_{yw} = 0$) and that the bank angle is a clockwise rotation about the velocity vector. The condition $\eta_{yw} = 0$ implies zero sideslip for a fixed wing aircraft and some nonzero sideslip for a single rotor helicopter due to the presence of the tail rotor.

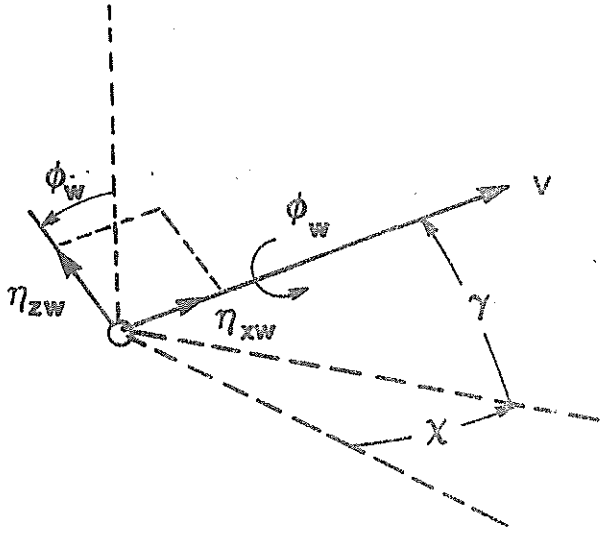

FIGURE 1. Flight Path Geometry

These wind axis equations are taken from fixed wing practice where it is straightforward to associate the limits on the external aerodynamic forces η_{xw} (thrust minus drag) and η_{zw} (lift) with power available and stall, respectively. The pilot has direct control over η_{zw} through elevator control of angle of attack and η_{xw} with thrust. For a helicopter the form is less convenient for studying maneuvers, especially at low speeds. However, it is a convenient form for expressing the maximum values of the available forces η_{xw} and η_{zw} in terms of power available for a rotorcraft. The orientation of the vehicle does not appear in these equations, but is implicit in the generation of the aerodynamic forces η_{xw} and η_{zw} by control action.

Limitations placed on the values of η_{xw} and η_{zw} due to installed power can now be examined. It is convenient to introduce the following normalization.
Define:

$$V_H = \left(\frac{W}{2\rho A}\right)^{\frac{1}{2}}$$

And then:

$$P_R^* = \frac{P_R}{W\,V_H} = \frac{P_R}{M\,P_H}; \qquad V^* = \frac{V}{V_H}; \qquad v^* = \frac{V}{V_H} \tag{2}$$

where M is the main rotor figure of merit.

η_{xw} and η_{zw} are the resultant aerodynamic forces acting on the helicopter, divided by weight. It is assumed that η_{zw} arises entirely due to the main rotor:

$$\eta_{zw} = \eta_{zR}$$

η_{xw} is the resultant aerodynamic force produced in the direction of flight less the airframe drag:

$$\eta_{xw} = \eta_{xR} - \frac{D_f}{W} \tag{3}$$

Thus, rectilinear level flight is given by $\eta_{zw} = 1$ and $\eta_{xw} = 0$.

Assuming, for simplicity, that the profile power is independent of rotor operating condition, the power required is expressed as:

$$P_R^* = P_{ip}^* + \left(\frac{1 - M}{M}\right) + \frac{1}{4}\frac{f}{A} V^{*3} \tag{4}$$

The total induced power plus the propulsive power above that for steady level flight can be written as:

$$P^*_{ip} = \eta_{xw} V^* + [(\eta_{xw})^2 + (\eta_{zw})^2]^{\frac{1}{2}} v^* \tag{5}$$

and the induced velocity is given by momentum theory as:

$$v^* = \frac{(\eta_{xw})^2 + (\eta_{zw})^2}{\sqrt{(P^{*2}_{ip} + V^{*2}\,\eta_{zw}{}^2)}} \tag{6}$$

Assuming that rotor RPM is constant, then:

$$P^*_R = P^*_{AV}$$

Thus the values of η_{xw} and η_{zw} available as a function of airspeed can be estimated using Eqs. (4) - (6) given the installed power, disc loading, figure of merit and fuselage drag. These values, combined with Eqs. (1), determine the flight path characteristics.

An energy equation can be obtained from the first of Eqs. (1) by multiplying by V dt and integrating to yield:

$$\left[\frac{V^2}{2} + gh\right]_f - \left[\frac{V^2}{2} + gh\right]_o = V_H g \int_o^{t_f} \eta_{xw} V^* \, dt \tag{7}$$

This formulation applies throughout the speed range of the helicopter, including hover. The simplicity of the formulation is obtained by two assumptions noted in the Appendix. The effect of steady level flight angle of attack is neglected in the momentum equation, while changes in angle of attack due to maneuvering are retained. Also, it has been assumed that $\eta_{xw} = \eta_{xR}$ in the induced power expression.

Note that a force normal to the flight path, η_{zw}, does not change the energy level of the helicopter and thus in an "ideal" loop or in fact any maneuver in which $\eta_{xw} = 0$:

$$\frac{V^2}{2} + gh = \text{constant} \tag{8}$$

In horizontal, wings-level flight, η_{xw} is equal to acceleration. Typical boundaries for maximum level acceleration and deceleration ($\eta_{zw} = 1$) are shown in Figure 2. The deceleration boundary is determined by the condition of zero power at high speeds and by maximum power at low speeds. Maximum translational acceleration is limited by installed power.

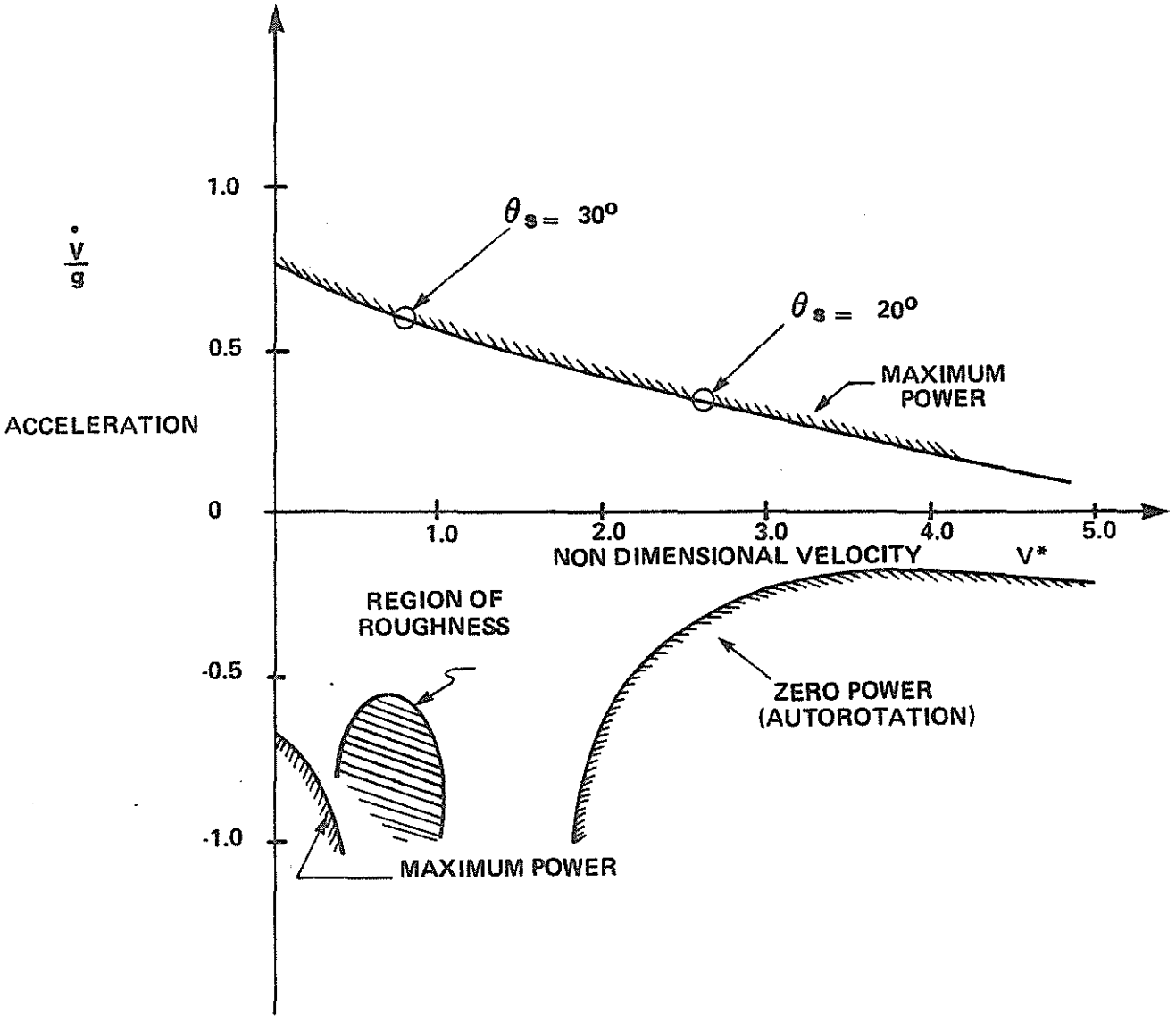

FIGURE 2. Rectilinear Flight Acceleration and Deceleration Boundaries

The variation in normal aerodynamic force (η_{zw}) with flight speed as a function of propulsive force (η_{xw}) is shown in Figure 3. As may be seen from equations (1), the propulsive force can be interpreted as corresponding to acceleration or climb. The maximum normal aerodynamic force attainable in constant speed level flight occurs near the speed for maximum effective lift-drag ratio of the rotorcraft for the parameters chosen for this example. The maximum value of η_{zw} occurs at the speed where:

$$\frac{\partial P^*_{Ro}}{\partial V^*} = \frac{P^*_A - P^*_{Ro}}{V^*} - 2\eta_{xw} \qquad (9)$$

At higher speeds, a considerable increase in the maximum normal force can be obtained by descent or deceleration. However, there is a rapid reduction in attainable normal force with climb or acceleration and the speed at which the maximum occurs decreases rapidly with climb angle as can be seen from Eq. (9) and the figure. Thus, the best performance in climbing turns tends to occur at a lower speed than that associated with maximum load factor.

The power relationship defines a surface of normal versus propulsive force as indicated, for example, in Reference (6). A cross section of this surface at a given flight speed is shown in Figure 4. The limitations on η_{xw} and η_{zw} can be used in conjunction with Eqs. (1) to determine the angular rates of the velocity vector which can be achieved.

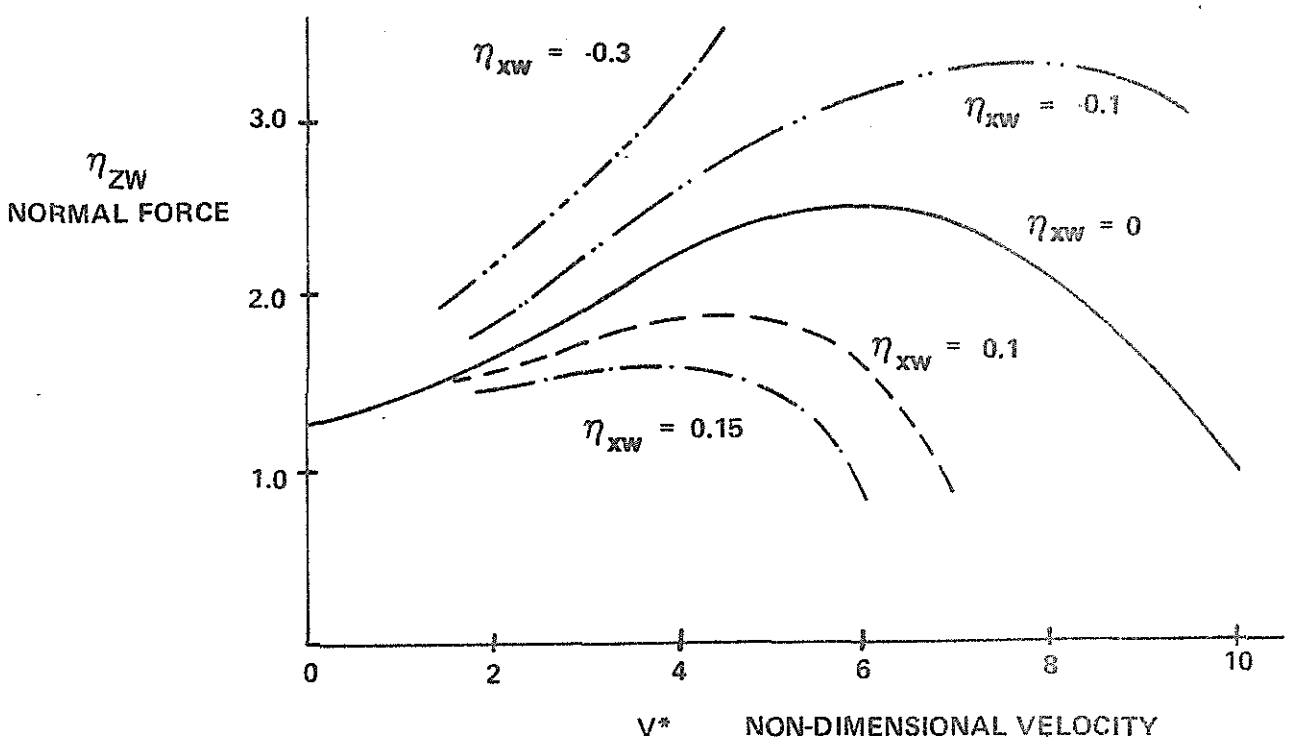

FIGURE 3. Influence of Propulsive Force and Normal Force Available at Maximum Power

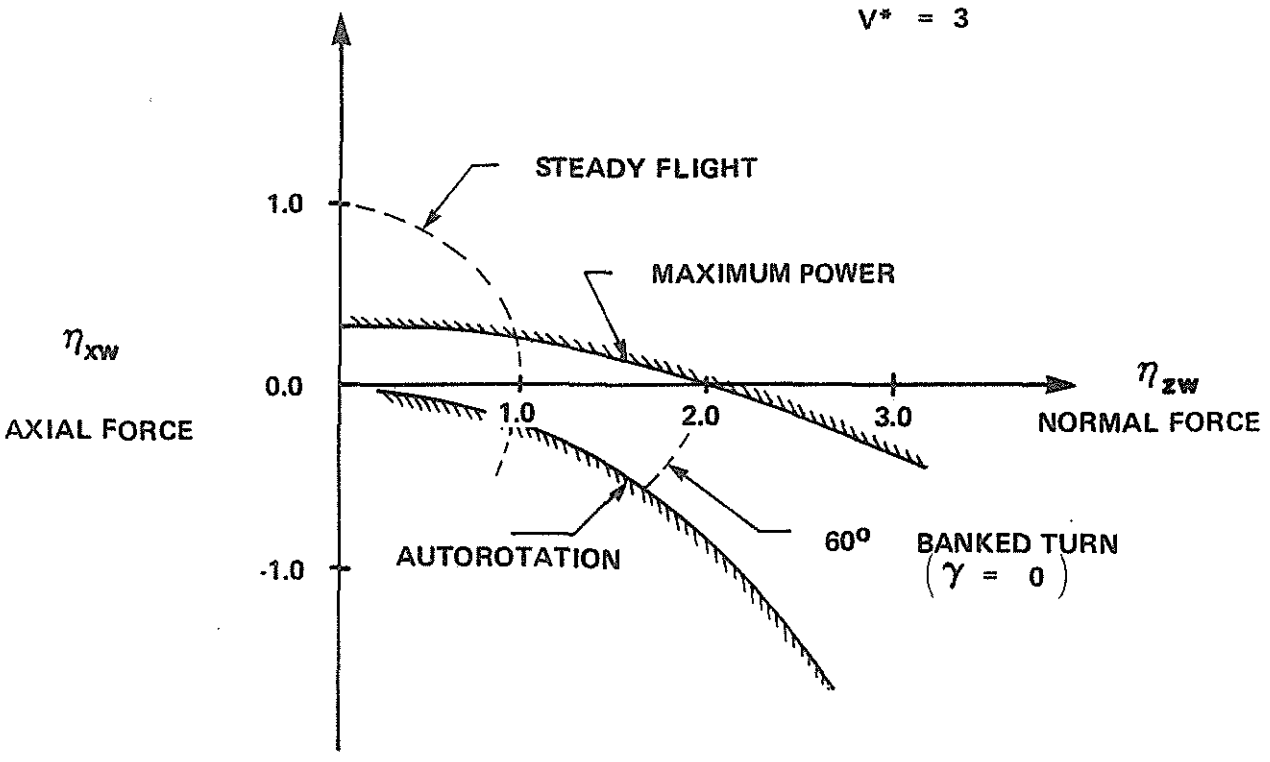

FIGURE 4. Aerodynamic Force Boundaries at a Given Flight Speed

5. Angular Rate Limits

If we consider η_{xw} and η_{zw} as control forces then Eqs. (1) may be used to determine angular rate limits. However, for the helicopter the connection between the forces and the controls available to the pilot needs to be accounted for. This is illustrated by the following simple examples. At low speeds, assuming that the primary force acting on the helicopter is rotor thrust, then:

$$\eta_{xw} = -\left(\frac{T}{W}\right) \sin\left(B_{1s} + \theta_s - \gamma\right)$$

$$\eta_{zw} = \frac{T}{W} \cos\left(B_{1s} + \theta_s - \gamma\right) \qquad (10)$$

Consider two limiting cases for the climb angle rate. In a symmetric pull-up with $\eta_{xw} = 0$, it can be shown from Eq. (7) that:

$$\dot{\gamma} = \frac{g}{V_H} \frac{(\eta_{zw} - \cos\gamma)^2}{V_o^* (\eta_{zw} - 1)}$$

$$V^* = \frac{V_o^* (\eta_{zw} - 1)}{(\eta_{zw} - \cos\gamma)} \tag{11}$$

These relationships indicate that as airspeed decreases the climb angle rate increases without limit. However, the condition that $\eta_{xw} = 0$ from Eq. (10) implies that:

$$B_{1s} + \theta_s = \gamma$$

Thus it is implied that the climb angle rate is equal to the pitch rate and so the limit on the applicability of Eqs. (11) depends upon the allowable pitch rate available from the longitudinal control. On the other hand, if a level body response is considered ($\theta_s = 0$), the solutions to Eqs. (1) yield:

$$\dot{\gamma} = \frac{g(\eta_z - 1)}{V_H V_o^*} \cos^2\gamma \tag{12}$$

$$V^* = \frac{V_o^*}{\cos\gamma}$$

This relationship also indicates that the initial climb angle rate increases without limit as airspeed decreases. However, this is a perfectly reasonable result since it essentially corresponds to a vertical acceleration at constant horizontal velocity ($\dot{\gamma} = -\dot{\alpha}$) and the very large angular rates are a consequence of the variables used to describe the motion. This is a transient value which will decay to a steady climb due to rotor vertical damping. Thus, at low speeds, it is necessary to be able to distinguish more detail regarding the maneuver performed and the controls applied. Two controls are available, the collective pitch and the longitudinal stick, and thus a moment balance as well as a force balance is required to examine the maneuvers possible.

Comparison of Eqs. (9) with flight test data on a high speed loop entry at $\eta_{zw} \cong 2$ are shown in Figure 5 indicating a constant energy maneuver.[2] Similar conclusions are obtained for maximum heading rate. That is for a level, constant speed turn ($\eta_{xw} = 0$), Eqs. (1) give:

$$\dot{\chi} = \frac{g}{V_H} \frac{\sqrt{\eta_{zw}^2 - 1}}{V_o^*} \tag{13}$$

Again no limit on heading rate is indicated with decreasing flight speed as shown in Figure 6, since the installed power permits $\eta_{zw} > 1$ in hover. However, the condition $\eta_{xw} = 0$ implies that the body yaw rate is equal to the heading rate, i.e., the maneuver is coordinated and the limit of the heading rate is governed by the maximum yaw rate available from the tail rotor as well as the pitch control when the aircraft is banked. If the body yaw rate is zero then:

$$\dot{\chi} = \frac{g\sqrt{\eta_{zw}^2 - 1}}{V_o} \cos^2\chi \tag{14}$$

and large initial heading rates are possible. Equation (14) corresponds to lateral acceleration with a fixed body attitude ($\dot{\chi} = \dot{\beta}$), maneuver possible at low speeds and again is a possible maneuver at low speeds limited by bank angle or maximum lateral velocity rather than power. The maximum body yaw rate available from tail rotor control inputs is large at low speed and decreases with airspeed due to sideslip limitations.

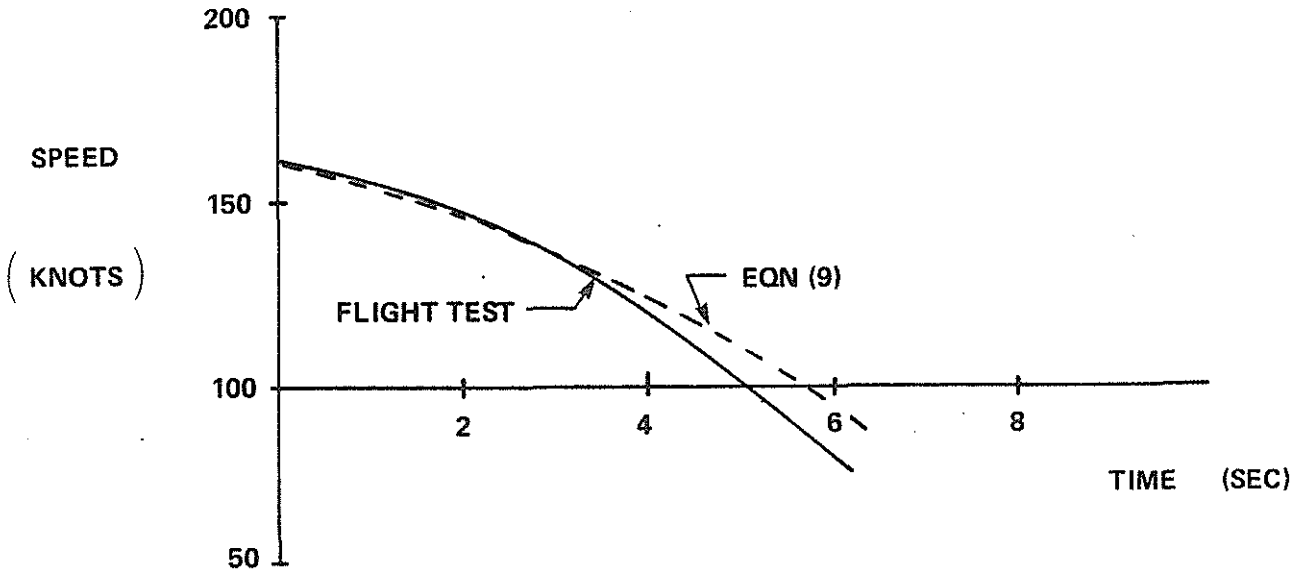

FIGURE 5. Entry into 2-g Loop Compared with Equation (9)

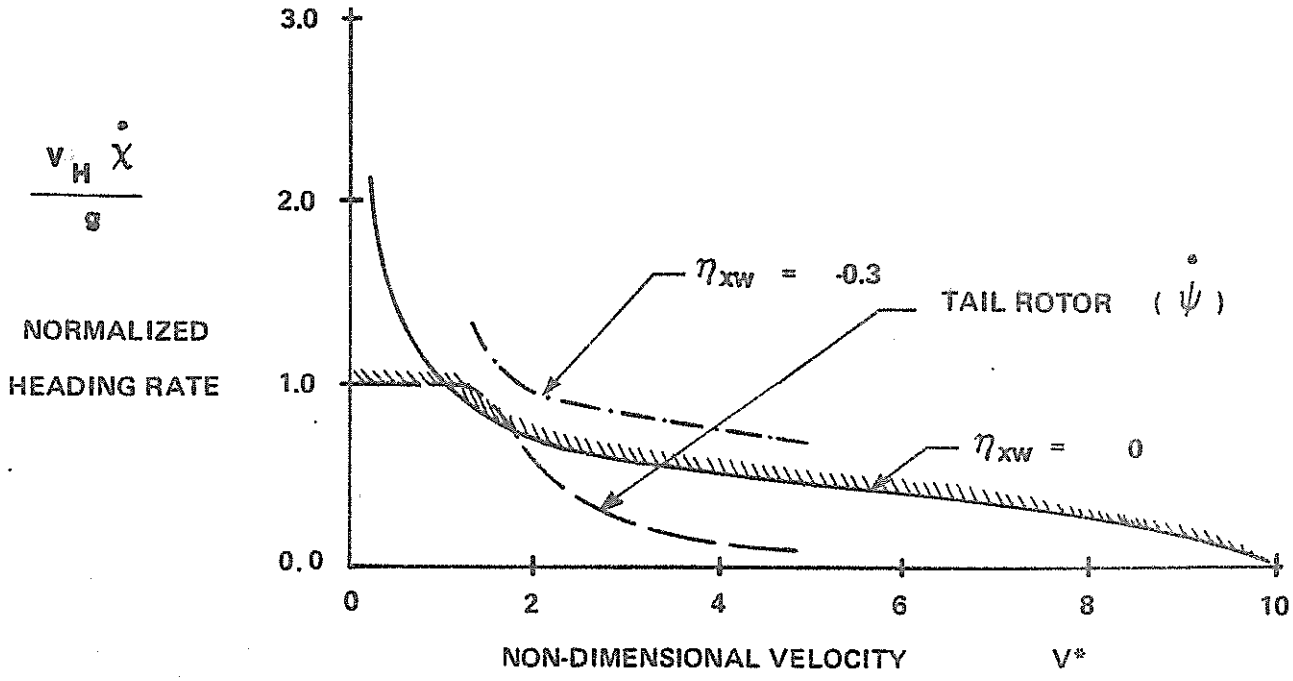

FIGURE 6. Heading Rate at Maximum Power and Yaw Rate

The equivalence of turn rate and body yaw rate in a coordinated maneuver leads to an interesting observation because of the nature of the tail rotor. The maximum body yaw rate allowable from the tail rotor decreases at high airspeeds due to sideslip limitations. This is illustrated in Figure 6. At low speeds, then, the tail rotor governs the maximum angular rate available in coordinated maneuvers. At high speeds the allowable η_{zw} governs the limit. Thus at low speeds it is convenient to consider coordinated turning as the reverse of the usual case. That is, the tail rotor control produces body yaw rate and the bank angle required to produce an equal heading rate is:

$$\phi_w = \tan^{-1}\left(\frac{V\dot{\psi}}{g}\right) \tag{15}$$

In hover, no bank angle is required and the application of tail rotor will produce a vehicle yaw rate. At low speeds, if no bank angle is applied, the helicopter rotates with the translational velocity remaining approximately fixed in space with sideslip varying. If there are no sideslip limitations, then the yaw rate and the heading rate are independent and large heading rates are possible as indicated by Eqn. (13).

It can now be clearly seen that, when using Eqn. (1), the assumption that $\eta_{xw} = 0$ essentially implies that the body rates and the velocity vector rates are the same. In this case the low speed limits on heading rate and climb angle rate are determined by the control limits on vehicle body pitch rate and yaw rate. Maneuvers with fixed body orientation at low speeds are possible and limits on heading rate

and climb angle rate are high and a result of the coordinate system used. To fully reflect these features of helicopter flight it is necessary to consider models with additional coordinates and it is desirable to employ a body axis system as described later in the paper.

6. Agility

In this section the influence of the control characteristics of the helicopter on achieving the limiting values of acceleration defined by the installed power will be examined. It has already been noted that, above a critical flight speed, the ability to re-orient the velocity vector is primarily a function of the normal acceleration available, while below this flight speed the ability to turn or pull up is limited by the control effectiveness. It has also been seen that an axial force variation along the flight path is required to change the energy state of the helicopter.

Recalling the relationships between the thrust vector of the helicopter and the wind forces η_{xw} and η_{zw}, Eqs. (10), it is seen that the energy state of the conventional helicopter is altered by changing body attitude. To accelerate or decelerate in level flight ($\gamma = 0$) without an auxiliary thruster, the following relationship applies:

$$\dot{V} = g\,\eta_{xw} \cong -\,g\,(\theta_s + B_{ls}) \tag{16}$$

Thus, acceleration is related directly to body pitch attitude. The longitudinal control produces a pitch rate which must be integrated to produce a pitch attitude. The time required to achieve a longitudinal acceleration is primarily a function of the steady pitch rate produced by the controls rather than the time constant in pitch as shown in Figure 7. Dooley has note a similar behavior in Reference 3. A thrusting device would give the pilot direct control over η_{xw}, consequently body attitude changes would not be required. For a tilt rotor aircraft accelerating with level body attitude, θ_s can be interpreted as rotor tilt angle. This implies that high tilt rates will be required to achieve horizontal acceleration rapidly. Reference 4 indicates pilot allowable body pitch rates are about 20°/sec.

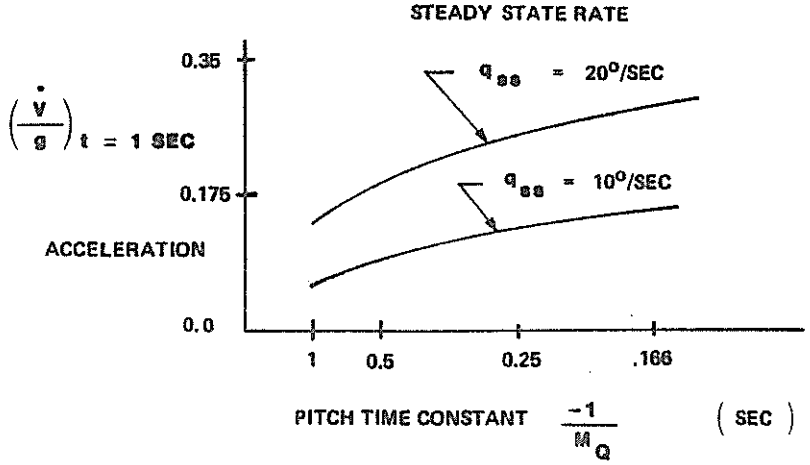

FIGURE 7. Acceleration After One Second as a Function of Pitch Time Constant and Steady State Rate

Additionally, depending upon the initial state of the rotorcraft, portions of the acceleration boundary are unavailable. Figure 8 shows acceleration from hover vs. time and also illustrates the acceleration boundary. This emphasizes the importance of pitch rate in achieving the maximum acceleration and that rotor hinge restraint is not of primary importance in achieving longitudinal acceleration.

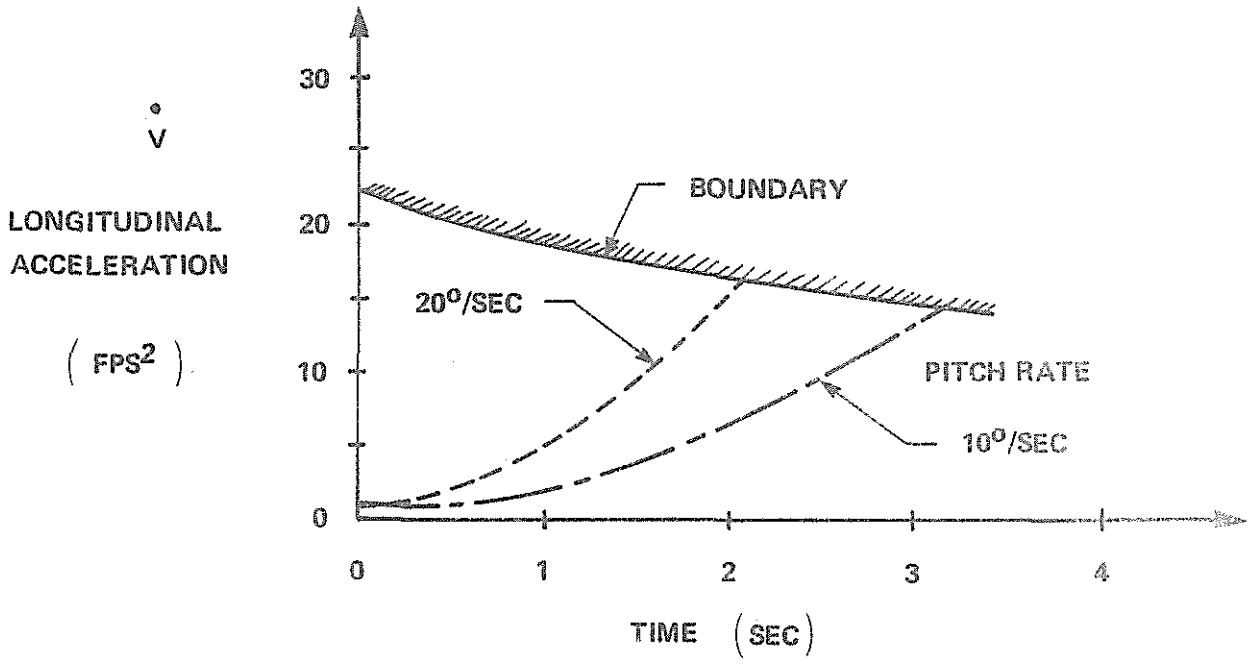

FIGURE 8. Approach to Longitudinal Acceleration Boundary as a Function of Pitch Rate

The deceleration limits indicated in Figure 2 are moderately low at high speeds and tend to increase to very large values at low speeds for straight line flight. Note that, in fact, the deceleration limit is the zero-power (autorotative) condition at higher speeds and then becomes the installed power limit at lower speeds. The values are such that there is essentially no limit on deceleration at low speeds associated with the vehicle parameters. Reference 5 supports this conclusion showing that the deceleration capability predicted for an OH-58 is essentially independent of installed power. Factors such as acceptable body attitude and proper coordination of controls will limit deceleration. Flight test results such as Reference 6 generally support the conclusion that the maximum acceleration and deceleration rates attainable are limited to values below those associated with vehicle parameters. At higher speeds, the deceleration rate may be increased by sideslipping to increase fuselage drag or turning with increased load factor, permitting a larger incidence for autorotation as also shown in Figure 9.

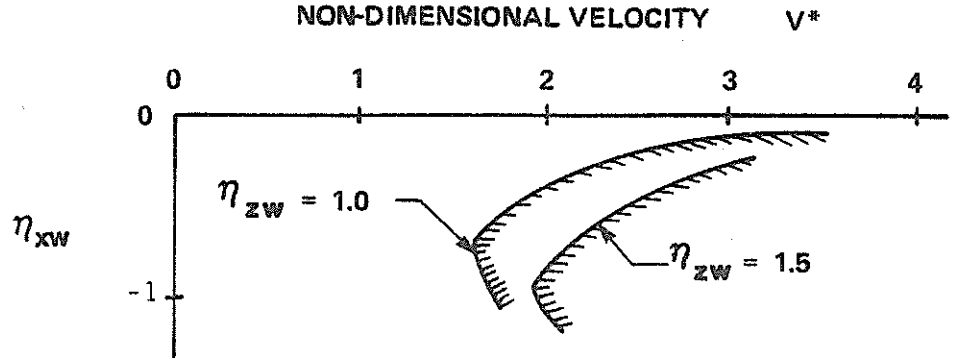

FIGURE 9. Deceleration as a Function of Normal Acceleration in Autorotation

Large accelerations and decelerations are directly associated with large body attitudes. In many tactical situations large body attitudes are undesirable as described, for example, in Reference 7. This reference states that "the ability to accelerate and decelerate without pitching would drastically reduce pilot workload", and also implies that an acceleration/deceleration capability of the order of 0.3 g's is desirable. This leads to the conclusion that direct horizontal thrust control is desirable. Direct horizontal thrust control could also be used to improve hovering control.

Another question of considerable interest in the agility of a helicopter is the time required to reverse direction. It has been seen that, in general, decreasing airspeed results in an increasing turn rate (and body yaw rate). This tends to indicate that the fastest turn around is achieved by decelerating while turning. Deceleration increases the allowable load factor, as shown earlier, and the lowered speed produces a faster turn rate at the same bank angle. The limit to this maneuver is probably governed by allowable attitudes and pilot technique rather than physical limitations of the aircraft. Under some circumstances the fastest way to do a 180° turn may be to decelerate to a sufficiently low speed that full pedal can be applied and then turn rapidly in an uncoordinated maneuver. Reference 4 gives allowable attitudes and rates as perceived by pilots indicating that considerably higher yaw rates are permissable near hover (55°/sec) compared to translational flight (15°/sec). This tends to support the fact that the fastest turn will be obtained by first decelerating in rectilinear flight to a very low speed and then applying full tail rotor control. In order to study this type of maneuver and other associated maneuvers it was considered desirable to develop a relatively simple simulation which would make it possible to investigate these various limitations.

7. Simulation Studies

The wind axis formulation discussed in the first part of the paper is convenient for examining the boundaries on available values of the aerodynamic forces and some of the limitations on dynamic maneuvering. However, it does not account for the manner in which these forces are generated by the control system of the helicopter. It is difficult, with the wind axis equations, to treat the fact that the helicopter possesses control of the normal aerodynamic force η_{zw} directly through collective pitch and indirectly through longitudinal control which produces a pitch rate and an angle of attack change. The angle of attack change alters η_{zw} through the rotor lift curve slope. However, the body attitude changes produced by these controls differ.

At low speeds, the vertical force, or collective, control produces little fuselage attitude change due to the absence of angle of attack stability, M_w. As the translational speed increases, if the helicopter exhibits a stable angle of attack stability, the vertical force control produces a body attitude change. In effect then, the force and moment controls become similar in that both produce a flight path rate as well as a pitch attitude rate. The response of the helicopter becomes similar for both controls and it may be less important to distinguish between these control inputs as is implied when using simplified models such as Eq. (1) considering η_{zw} and η_{xw} as control inputs.

Typical control relationships in the vertical plane are illustrated in Figure 10. The flight path rate limit is obtained from the installed power. This value can be achieved in a transient due to collective application, and then will decay due to vertical damping to steady climb ($\dot{\gamma} = 0$) and is important in a maneuver such as a bob-up. If the vehicle possesses angle of attack stability, the flight path rate will decay to a small value at low speeds. As airspeed increases and consequently M_w increases, the rate will approach the power limited value. Application of longitudinal stick will produce a steady pitch rate and an associated equal flight path rate. The pitch rate will be limited by the control system. The figure shows, as an example, the case in which the longitudinal control cannot generate the power limited value of η_{zw} at lower speeds.

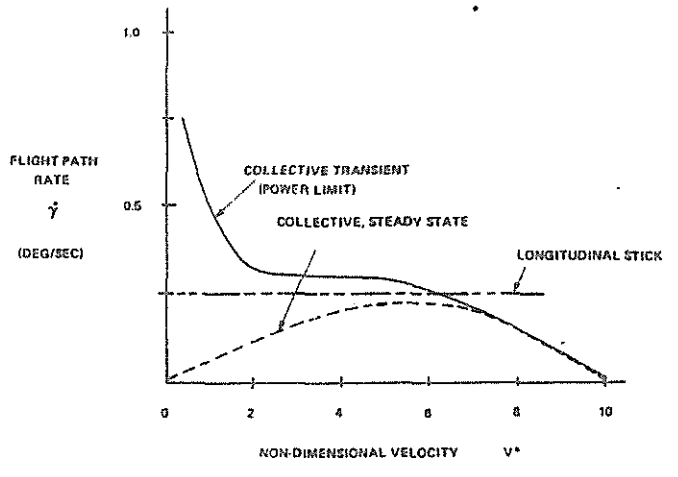

FIGURE 10. Typical Limits on Flight Path Rate

At high speeds, the actions of the collective and longitudinal stick become equivalent. A similar independence exists for the lateral/directional axes at low speeds where the lateral control of bank produces a heading rate but little change in body rate and the tail rotor produces body rate but little change in the heading rate due to the weak side force characteristic. As the speed increases the directional stability of the vehicle will increase and it becomes reasonable to assume that a bank angle produces heading rate as well as a body turn rate. In some studies it may be satisfactory to assume perfect coordination.

A simplified set of equations has been developed to properly reflect these features of the mechanics of flight which allows independence of body motion and flight path motion permitting uncoordinated flight as well as coordinated flight at non-zero sideslip. Emphasis was placed on retaining only the dominant features of helicopter maneuvering noted. While it is realized that considerably more complex models could be developed, it was considered that the equations of motion described below could be used to identify the dominant parameters associated with the maneuvering of helicopters.

A set of conventional body axis equations is employed. No small angle assumptions are made and so the conventional Euler angle relationships are used. In the simplest form the equations of motion are:

$$\dot{U} + g \sin\theta = X_u(U) + X_{\delta_T} \delta_T$$

$$\dot{V} + UR - g \cos\theta \sin\phi = Y_o(U) + Y_v V \qquad (17)$$

$$\dot{W} - UQ - g \cos\phi \cos\theta = Z_o(U) + Z_w W + Z_{\theta_c} \delta_{\theta_c}$$

$$M_w W + M_Q Q + M_{\delta_p} \delta_p = 0$$

$$N_v V + N_R R + L_{\delta_{TR}} \delta_{TR} = 0$$

$$L_v V + L_p P + L_{\delta_A} \delta_A = 0$$

The body rate Euler angle relationships are:

$$\dot{\theta} \cos\phi + \dot{\psi} \cos\theta \sin\phi = Q$$

$$\dot{\psi} \cos\theta \cos\phi - \dot{\theta} \sin\phi = R \qquad (18)$$

$$\dot{\phi} \cong P$$

In this form, the angular time constants have been neglected. They can, of course, be readily incorporated in the moment equations. They are likely to be of importance and will be incorporated in later studies. The terms $X_u(U)$, $Y_o(U)$, $Z_o(U)$ provide simplified trim behavior; $X_u(U)$ for attitude vs. airspeed, $Y_o(U)$ for non-zero trim sideslip and $Z_o(U)$ to represent the collective variation with airspeed in level flight. Various inertial terms were assumed to be small for simplicity. The angular damping and control sensitivity terms were assumed independent of airspeed and the directional stability and angle of attack stability were assumed stable and proportional to the velocity U. Control inputs include longitudinal thrust δ_T, collective δ_{θ_C}, longitudinal stick δ_p, lateral stick, δ_A and tail rotor δ_{TR}. These equations were considered to represent the simplest possible formulation of the equations of motion of a helicopter which permit hovering, forward, rearward, and sideward flight and permit investigation of large amplitude maneuvering. This model, with the assumptions regarding the variation of directional stability and angle of attack stability with translational velocity, gives the basic relationships desired for the action of lateral control, tail rotor, collective and longitudinal control indicated by Figures 6 and 10. Control power effects can be readily examined by limiting the allowable magnitudes of the control deflections. These equations serve as a useful starting point for studies of maneuverability and agility. Additional complexity can be readily added.

These equations of motion were programmed on a small digital computer and the output used in conjunction with an Evans and Sutherland multi-picture video display system. The display consists of three sections as shown in Figure 11. The upper third of the display gives a plan view of the two helicopters, the center third gives a view out the cockpit and the lower third has representations of various instruments. Two display units are available such that experiments can be flown with two independent aircraft. Cyclic and collective control sticks are used to apply inputs to the real time simulation. It is challenging to fly and experienced pilots have commented favorably on its essential realism. Preliminary results have shown the importance of body attitude and indicated the disadvantages of conventional control methods where acceleration is achieved by body attitude.

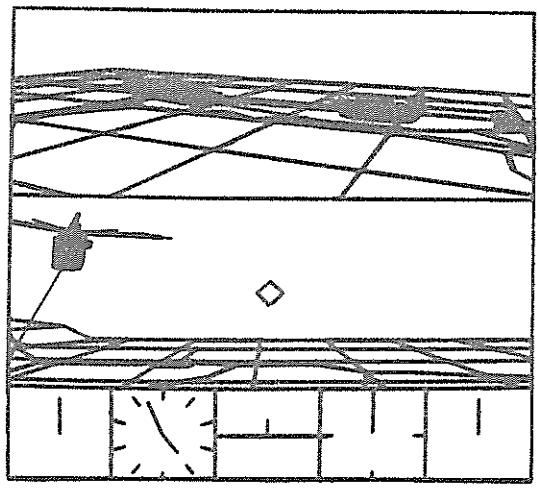

FIGURE 11. Evans and Sutherland Video Display

8. Conclusions

1. Highly simplified, three-degree of freedom, point-mass models are satisfactory approximations for rotorcraft simulation at high speeds. However, they do not account for the unique low speed, uncoordinated maneuver capabilities of rotorcraft.

2. A simple, six-degree of freedom (force and moment balance) body axis formulation has been developed which realistically simulates the control action and motion of rotorcraft at low speeds, including hover, sideward, and rearward flight.

3. The approach of expressing the total induced power and additional propulsive power required for maneuvering in terms of the horizontal and vertical load factors permits the calculation of total power required as a function of maneuver state or the determination of maneuver limits as a function of vehicle design parameters.

4. Coordinated flight at low speeds is limited by tail rotor control power. Uncoordinated flight is constrained by various factors in addition to available power, such as allowable body attitudes.

5. In many maneuvers it may be that the level of attainable accelerations and turn rates are governed by the limits placed on body attitudes and rates by the pilot, and not those associated with vehicle parameters. Therefore, simulations have a valuable role in quantifying the effectiveness of design concepts, but must accurately represent the rotorcraft's unique low speed characteristics.

9. Notation

A	rotor disc area, ft^2
D_f	parasite drag of rotorcraft, lbs
f	equivalent flat plate area of rotorcraft, ft^2
h	altitude, ft
M	main rotor figure of merit
N_{xw}	component of main rotor force along flight path, positive in direction of flight, lb
N_{zw}	component of main rotor force normal to flight path, positive up, lb
N_{xw}	resultant aerodynamic force along flight path, referred to as propulsive force, lb
N_{zw}	resultant aerodynamic force normal to flight path, referred to as normal force, lb
P_R	power required, hp
P_{AV}	power available to main rotor, hp
P_{ip}	induced power plus propulsive power above that required for steady, level flight, hp
V	resultant flight velocity, fps
V_H	reference velocity, fps
v	induced velocity, fps
η_{xw}	resultant aerodynamic force along flight path normalized by weight
η_{zw}	resultant aerodynamic force normal to flight path normalized by weight
γ	flight path angle
χ	heading
Φ_w	bank angle about velocity vector
θ_s	body pitch attitude
ψ	body yaw attitude
B_{1s}	longitudinal cyclic pitch
$(\ )_o$	steady level flight
$(\ )^*$	normalized quantities

10. References

1. Wood, T. L., Ford, D. G., Brigman, G. H., Maneuver Criteria Evaluation Program, USAAMRDL Technical Report 74-32, May 1974, AD782209.

2. Falco, M. and Smith, R., Influence of Maneuverability on Helicopter Combat Effectiveness, NASA Conference Publication 2219, Helicopter Handling Qualities, April 1982.

3. Dooley, L. W., Handling Qualities Considerations for NOE Flight, Journal of the American Helicopter Society, Vol. 22, No. 4, October 1977.

4. Dooley, L.W., Rotor Blade Flapping Criteria Investigation, USAAMRDL-TR-76-33, December 1976, AD034459.

5. Merkley, D. J., An Analytical Investigation of the Effects of Increased Installed Horsepower on Helicopter Agility in the Nap-of-the-Earth Environment, USAAMRDL-TN-21, December 1974.

6. Wells, C. D. and Wood, T. L., Maneuverability - Theory and Application, Journal of the American Helicopter Society, Vol. 18, No. 1, January 1973.

7. Legge, P. J., Fortescue, P. W. and Taylor, P., Preliminary Investigation Into the Addition of Auxiliary Longitudinal Thrust on Helicopter Agility, Paper Presented at the Seventh European Rotorcraft Forum, September 1981.

11. Appendix

The power required for the main lifting rotor can be written in terms of the resultant forces acting on the rotor parallel and perpendicular to the flight velocity of the rotor (N_{xR}, N_{zR}) as

$$P_R = N_{xR} V + (N_{xR}^2 + N_{zR}^2)^{\frac{1}{2}} v + P_o \tag{A-1}$$

where P_o is the profile power and v is the induced velocity.

The resultant aerodynamic force balance in the direction of the wind can be written for the complete helicopter as:

$$N_{xw} = N_{xR} - D_f \tag{A-2}$$

and

$$N_{zw} = N_{zR}$$

where D_f is the drag of all of the components of the helicopter.

It is assumed that the induced velocity is given by momentum theory:

$$v = \frac{(N_{xR}^2 + N_{zR}^2)^{\frac{1}{2}}}{\sqrt{(v - V \sin\varepsilon)^2 + (V \cos\varepsilon)^2}} \tag{A-3}$$

In this case,

$$\sin\varepsilon \cong \frac{N_{xR}}{(N_{xR}^2 + N_{zR}^2)^{\frac{1}{2}}}$$

$$\cos\varepsilon \cong \frac{N_{zwR}}{(N_{xR}^2 + N_{zR}^2)^{\frac{1}{2}}} \tag{A-4}$$

The induced velocity can be expressed in terms of N_{xR} and N_{zR} using (A-4). In the propulsive term in Eqn. (A-1), N_{xR} is eliminated using equation (A-2). It is satisfactory to assume that $N_{xR} = N_{xw}$ since N_{xw} can take on large values compared to N_{xR} only at low speeds when the airframe drag is small and so $N_{xR} \cong N_{xw}$.

The resulting power equation is:

$$P_R = N_{xw} V + (N_{xw}^2 + N_{zw}^2)^{\frac{1}{2}} v + P_o + P_f \tag{A-5}$$